Universiteit
Leiden
The Netherlands

Synthetic modifications of the antibiotic peptide gramicidin S : conformational and biological aspects

Knijnenburg, A.D.

Citation
Knijnenburg, A. D. (2011, September 29). *Synthetic modifications of the antibiotic peptide gramicidin S : conformational and biological aspects*. Retrieved from https://hdl.handle.net/1887/17882

Version:	Corrected Publisher's Version
License:	Licence agreement concerning inclusion of doctoral thesis in the Institutional Repository of the University of Leiden
Downloaded from:	https://hdl.handle.net/1887/17882

Note: To cite this publication please use the final published version (if applicable).

8

Summary and future prospects

The research described in this thesis focuses on synthetic modifications of the antibiotic peptide gramicidin S (GS). The aim of the research is the development of non–toxic analogs of GS using conformational and amphipathic changes induced by sugar amino acids (SAAs) and/or non–proteinogenic amino acids. A short overview of clinically applied antibiotics during the past decades is presented in **Chapter 1**, combined with the introduction of GS. In addition, modifications of the ring–size of GS and the use of dipeptide isosteres in GS analogs are discussed.

In **Chapter 2** an oxetane (**1**), furanoid (**2**) and pyranoid (**3**) SAA are used as dipeptide isosteres of the type II' β–turn of GS.[1] By the introduction of these varying ring–size SAAs the span of the type II' β–turn is gradually increased (Figure 1). The effect of these modifications are studied by molecular modeling, which reveal that the pyranoid SAA **3** is the best fit for the type II' β–turn of GS. By CD and NMR it was shown that the secondary structures of GS**1**–**3** exhibit solvent dependence and that they are not as rigid as the naturally occurring GS. GS**1**–**3** are all less hydrophobic than GS and exhibit lower toxicity towards

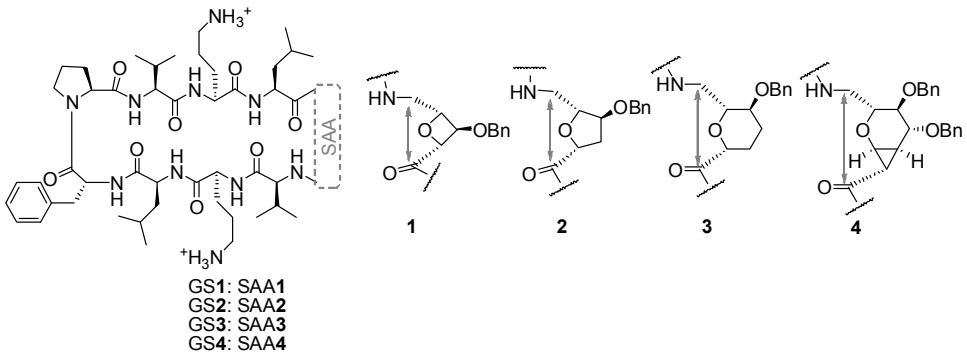

Figure 1: GS analogs (GS**1**-**4**) with SAA **1**-**4** modified turn regions. The grey arrows indicate the increasing distance between the carboxyl and aminomethyl substituents.

mammalian cells. GS**1** and GS**2** are also less active in killing micro–organisms; GS**3** on the other hand is promising, because it shows a similar antimicrobial activity as GS in addition to the lower toxicity. Thus, the incorporation of SAAs at the type II' β-turn of GS are of interest in making subtle changes in the overall hydrophobicity and the conformation of the molecule. The correlation between flexibility and biological activity is an interesting subject for future research. CD measurements using unilamellar phospholipid vesicles that mimic either the mammalian cell membrane or the bacterial cell membrane might give insight in the behavior of GS analogs on the lipid bilayer.[2]

By increasing span of the SAAs a better biological profile was observed in **Chapter 2** being SAA **3** the best fit for the type II' β–turn. Following this trend, another interesting modification of the β–turn is the incorporation of SAAs with a larger span than that of SAA**3** which might improve the biological activity. This is exemplified by the oxabicyclo[4.1.0] heptane SAA **4** which has an additional cyclopropane ring attached to the pyranoid ring. The hypothesis is tested by synthesizing GS**4**, measuring the NMR and testing the biological activity. The $^{3}J_{HN\alpha}$ and $\Delta\delta H_{\alpha}$ show that GS**4** is less able to form a β–sheet/β–turn structure than GS (Figure 2, $^{3}J_{HN\alpha} < 7$and $\Delta\delta H_{\alpha} < 0.1$ for Val, Leu and Orn). Additionally, the

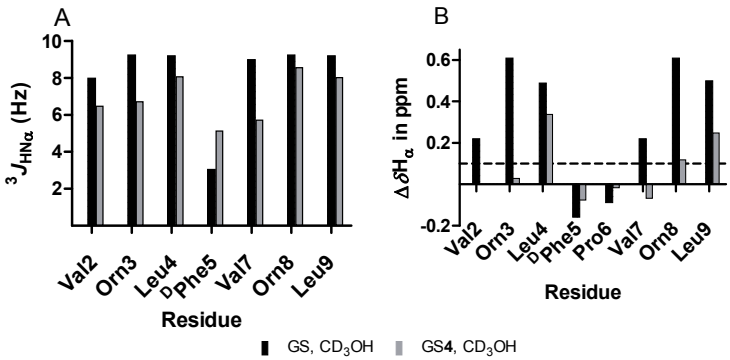

Figure 2: [A] $^{3}J_{HN\alpha}$ and [B] $\Delta\delta H_{\alpha}$ of GS and GS**4**.

antimicrobial activity tested against a standard panel of Gram–positive and Gram–negative bacteria reveal that GS**4** has both a lower bactericidal and hemolytic activity (see Table 1, Experimental section).

Chapter 3 describes the incorporation of the series of furanoid SAAs **5**–**7** in the turn region of tetradecameric GS analogs (Figure 3).[3] The incorporated SAAs have an altered substitution pattern with either a fully hydroxylated, mono–benzylated or di–benzylated carbohydrate core and the hydrophobicity is in this way varied in the turn region. Conformational analysis with NMR and CD show that all the analogs have a slight distortion of the β–hairpin structure in comparison with the tetradecameric template (*cyclo*-(VOLOV^{D}FPLOVOL^{D}FP)). Interestingly, the new analogs (GS**5**–**7**) exhibit high antimicrobial activity against Gram–positive and Gram–negative bacteria and a lower toxicity towards mammalian cells (especially GS**5**) compared with the template, but are still more toxic than GS.

To overcome the toxicity of GS**5**–**7** it was envisaged that the substitution of a L-amino acid into a D–amino acid, such as D–ornithine, would lead to a modified amphipathic character, which was studied in **Chapter 4**.[4] X–ray analysis of a tetradecameric GS analog (*cyclo*-(VKL^{D}KV^{D}YPLKVKL^{D}YP)), show that the cationic amino acid indeed is situated on the apolar surface of the molecule. The SAAs **5**–**7** were incorporated as a turn mimic in the tetradecameric template (*cyclo*-(VOL^{D}OV^{D}FPLOVOL^{D}FP)), which resulted in GS**8**–**10**. The whole series (GS**5**–**10**, Figure 3) was subjected to a detailed conformational study which showed that all analogs are capable of making a β–hairpin structure albeit not with the same stability as the templates in various solvent systems. The different substitution patterns of the SAAs create a series of decreasing hydrophobicity going from GS**5**-GS**10**. It became apparent that the less hydrophobic analogs are less toxic. GS**10** is also less active in killing micro–organisms, but GS**8** and GS**9** show a promising therapeutic profile: less toxic than GS but with retained antimicrobial activity. The overall hydrophobicity of the tetradecameric analogs can be tuned via incorporation of functionalized SAAs or D–amino acids at specific positions. The

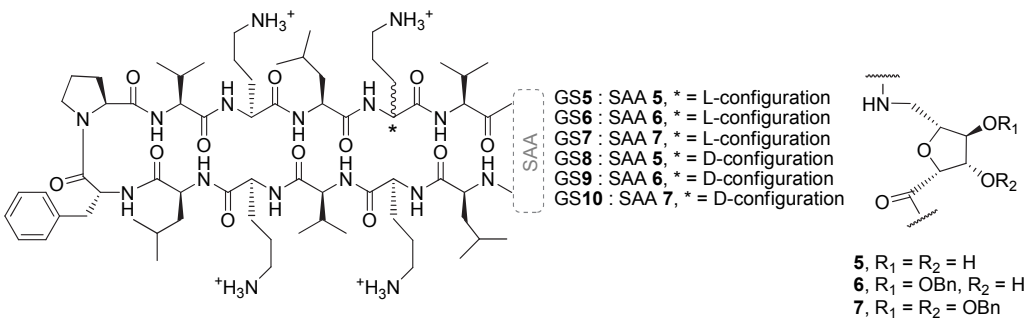

Figure 3: GS analogs (GS**5**-**10**) with SAAs **5**-**7** modified turn regions.

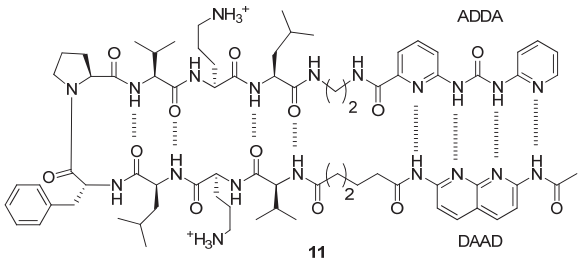

Figure 4: Acyclic β-hairpin **11** with hydrogen bond motifs ADDA and DAAD (D = hydrogen bond donor, A = hydrogen bond acceptor.

results imply that both hydrophobicity and flexibility are important factors in the development of less toxic GS analogs. It would be fruitful to test these compounds on phospholipid model membranes mimicking mammalian or bacterial membranes to see which conformational changes of the peptides are occurring during the lysis of the lipid bilayer.[5]

More flexibility into GS analogs can be created by the synthesis of acyclic variants of GS. However, acyclic GS analogs have thus far proved to be random coiled in solution and therefore inactive in killing micro–organisms.[6] In order to obtain an acyclic β–hairpin structure, it is hypothesized that complementary hydrogen bond motifs (DAAD and ADDA) may stabilize the acyclic β–hairpin (**11**, Figure 4). An additional feature of hydrogen bond motifs is that they can form strong dimers in an apolar environment, but have a weaker interaction in an aqueous environment.[7] It is hypothesized that this feature might lead to selective lysis of the bacterial membrane, which is far more apolar than the mammalian cell membrane.[8]

To confirm these hypotheses analog **11** was synthesized via a safety catch method on solid phase (Scheme 1). First, the safety catch resin **12** was loaded with Fmoc-L-leucine (**13**) and subsequent automated solid phase peptide synthesis gave octamer **14**. Hydrogen bond motif **17**[9] was coupled to resin **14** and the resin was alkylated with iodoacetonitril resulting in resin **16**. Subsequently resin **16** was susceptible for nucleophilic attack by hydrogen bond motif **20**. Motif **20** was obtained by an amide coupling of acid **18**[9] with mono–bocylated ethylenediamine (Scheme 1).

CD analysis shows that **11** is not capable of forming a β–hairpin in a methanol solution, though an enhancement of the Cotton effect is seen at 220 nm (typical wavelength of a β–sheet structure[10]) in going from water to methanol. The biological activity of analog **11** is rather poor. Compound **11** shows only minor activity against *S. epidermidis* and *B. cereus*, but exhibits low hemolytic activity (see Experimental section).

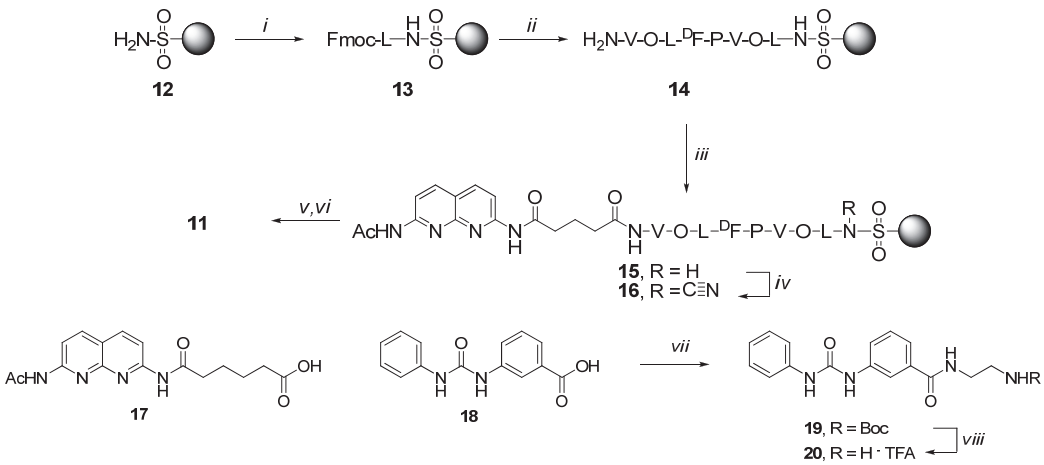

Scheme 1: Reagents and conditions: (*i*) Fmoc-Leu-OH, HCTU and DiPEA in 1:1 DCM/NMP; (*ii*) automated SPPS; (*iii*) **17**, HCTU, DiPEA; (*iv*) Iodoacetonitril, 5% DiPEA in NMP; (*v*) **20** in 20% DiPEA in THF; (*vi*) 95/2.5/2.5 TFA/TIS/H_2O (*vii*) mono-bocylated ethylenediamine, HCTU, DiPEA (*viii*) TFA/DCM, 1:1.

Increasing the hydrophobicity via the incorporation of SAAs with different ring–size or via hydrophobic substitutions at the carbohydrate core can have a beneficial effect on the biological profile (Chapter 2 and 3). In addition, changing the amphipathicity via the incorporation of a D–amino acid proves to be rewarding (**Chapter 4**). **Chapter 5** describes the combination of these strategies via the synthesis of tetradecameric GS analogs having an oxetane (**21**, **22**), furanoid (**23**, **24**) or pyranoid (**25**, **26**) SAAs incorporated at the turn region (Figure 5). The SAAs used were either non–benzylated or benzylated to result in turn mimics with increasing hydrophobicity. The SAAs **21**–**26** were incorporated both in the turn region of a tetradecameric GS analogs having only L–ornithines (GS**27**–GS**33**) and a tetradecameric GS analog having one D–ornithine substitution (GS**34**–GS**40**). NMR analysis showed that all resulting analogs were capable of forming cyclic β–hairpins in methanol. However, the analogs with D–ornithine appear to be very hydrophilic which is detrimental for the biological activity: GS**34**–**40** display only

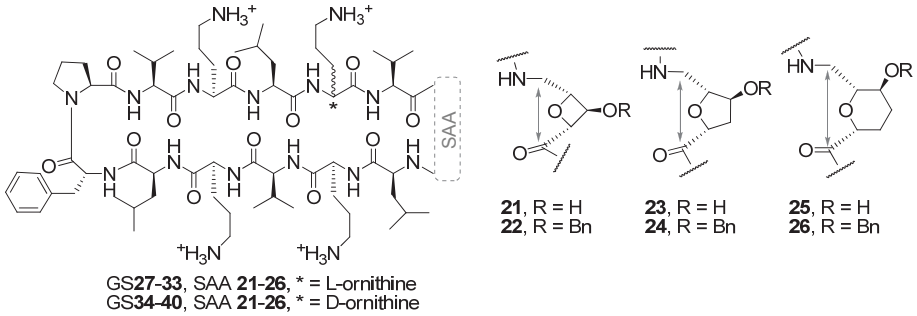

Figure 5: Tetradecameric GS analogs GS**27**-**40** with varying ring-size SAAs **21**-**26**.

minor antimicrobial activity against *S. eperdimidis* and very low hemolytic activity. On the other hand the peptide series GS**27**–**33** show high antimicrobial activity against both Gram–positive and Gram–negative bacteria. Peptides GS**27**–GS**33** were less toxic than the tetradecameric template, but still more toxic than GS.

Chapter 6 deals with "inverted" GS analogs having altered ring–size SAAs (**22**, **24** and **26**) in the turn region. "Inverted" GS analogs **42** and **43** have four cationic amino acids and two apolar adamantanyl amino acids in the β–sheet of the molecule (Figure 6) instead of two cationic amino acids and four apolar residues as in GS. In this way the amphipathicity is changed which has a beneficial effect on the biological activity. **42** and **43** are antimicrobially active against Gram–positive and Gram–negative pathogens and show lower hemolytic activity than GS (especially **42**). In this chapter the synthesis, conformational and biological evaluation is described of analogs GS**44**–**49** having different ring-size SAAs in the turn region of template **42** and **43**. Analog **46** with the pyranoid SAA as turn mimic shows the best β–hairpin structure in solution according to NMR and CD. It was shown that via the incorporation SAAs of different ring–size subtle changes are made in hydrophobicity of the peptides. GS**44**–**49** display high antimicrobial activity against both Gram–positive and Gram–negative bacteria, and show lower toxicity than GS.

The research described in **Chapter 7** entails the study of tuning hydrophobicity in tetradecameric GS analogs with adamantanyl amino acids. Amphipathicity is of great importance to create active GS analogs. The four hydrophobic amino acids valine and leucine are systematically replaced by adamantyl–L–glycine and adamantyl–L–alanine in a tetradecameric GS analog containing six cationic charges (**50**–**60**, Figure 7). In this way the hydrophobicity at the apolar face of the molecule is varied. According to the CD spectra the series **50**–**60** is well capable of forming a β–hairpin motif. All amino acid substitutions performed therefore result in a variation of amphipathic character. A trend is observed concerning the toxicity: the more hydrophobic the analog, the more

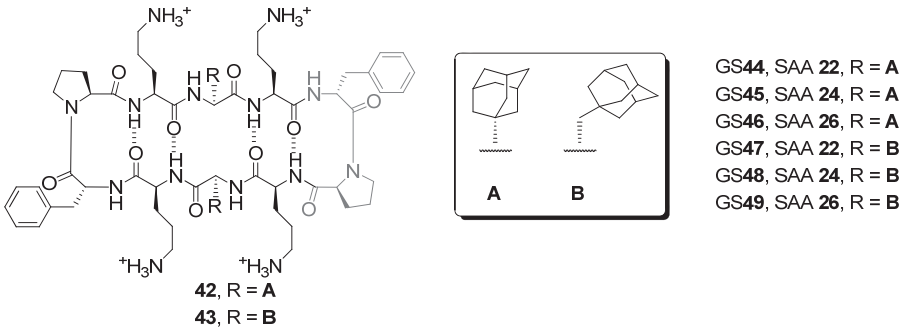

Figure 6: GS analogs having a SAA turn mimic (GS**44**-GS**49**) based on "inverted" GS analogs **42** and **43**.

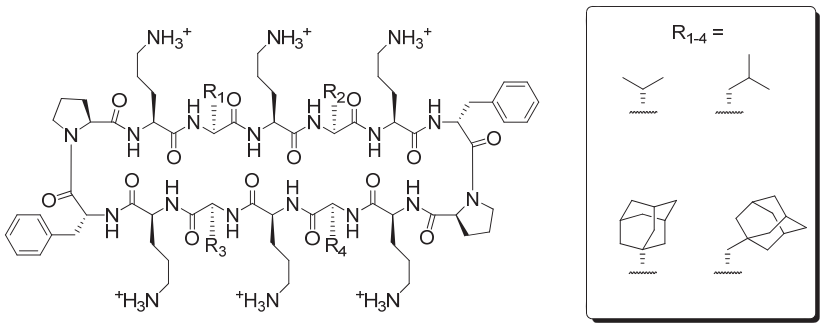

50-60

Figure 7: Tetradecameric GS analogs (**50**-**60**) with six cationic charges and the non-proteinogenic substitution of adamantane-L-glycine and adamantane-L-alanine.

hemolytic. Concerning the antimicrobial activity, a summit is seen: the compound at the outer limits of the hydrophobicity spectrum are not active and the analogs containing two adamantane substitutions are potently active against Gram–positive and Gram–negative bacteria. Unfortunately these compounds are more toxic than GS.

In conclusion, the research described in this thesis has analyzed the conformational and biological properties of modified GS derivatives and various derivatives appeared to be less toxic than GS. By the frequent use and misuse of antibiotics the amount of untreatable bacterial infections has increased. This research has contributed to the development of antibiotics for which resistance by bacteria should not easily occur.

Experimental section

General:

Light petroleum ether with a boiling range of 40 – 60 ºC was used. All other solvents used under anhydrous conditions were stored over 4Å molecular sieves except for methanol which was stored over 3Å molecular sieves. Solvents used for work–up and silica gel column chromatography were of technical grade and distilled before use. All other solvents were used without further purification. Reactions were monitored by TLC–analysis. The linear peptides were cleaved from resin, cyclized and purified by RP–HPLC (Gilson GX–281) with a preparative Gemini C18 column (Phenomenex 21.2 mmϕ x 150 mmL, 5µm particle size). The applied eluents were A: 0.1 % aq. TFA, B: MeCN. The linear peptides and cyclized peptides were analyzed with LC/MS (detection simultaneously at 214 and 254 nm) equipped with an analytical C18 column (4.6 mmϕ x 250 mmL, 5µm particle size). The applied eluents were A: H_2O, B: MeCN and C: 1.0 % aq. TFA. High resolution mass spectra were recorded by direct injection (2 µL of a 2 µM solution in H_2O/MeCN; 50/50: v/v and 0.1% formic acid) on a mass spectrometer Thermo Finnigan LTQ Orbitrap equipped with an electrospray ion source in positive mode (source voltage 3.5 kV, sheath gas flow 10, capillary temperature 523 K) with resolution R = 60000 at m/z 400 (mass range m/z = 150 – 2000) and dioctylphthalate (m/z = 391.28428) as lock mass. CD and hemolytic curves were analyzed with Graphpad Prism version 5.01 for Windows, GraphPad Software, San Diego California USA. IR spectra were recorded on a Perkin Elmer Paragon 1000 FT–IR Spectrometer.

Circular Dichroism Spectroscopy

CD spectra were recorded at 298 K on a Jasco J–815 spectropolarimeter using 0.1 cm path length quartz cells The CD spectra are averages of four scans, collected at 0.1 nm intervals between 190 and 250 nm with scanning speed 50 nm/min. The peptides were prepared at concentrations 0.1mM in 0.01 M NaOAc (pH 5.3) and 0.1 mM in MeOH. Ellipticity is reported as mean residue ellipticity [θ], with approximate errors of ± 10% at 220 nm.

Table 1: Cytotoxic (Hemolytic) and Antimicrobial Activity (MIC) of GS, GS**4** and **11**.

Analogsues	*Erythrocytes*[a]	*S. aureus*[b]	*S. epidermidis*[b]	*E. faecalis*[b]	*B. cereus*[b]	*P. aeruginosa*[c]	*E. coli*[c]
GS	31.2	4	2	8	4	64	32
GS**4**	125	32	8	>64	64	>64	>64
11	125	>64	32	>64	64	>64	>64

[a] Peptide concentration required for 100% lysis of erythrocytes in μM; [b] Gram-positive bacteria, MIC mg/L [c] Gram-negative bacteria, MIC mg/L. MW GS: 1369.49; GS**4**: 1490.63; **11**: 1737.84

Antimicrobial screening

The following bacterial strains were used: *Staphylococcus aureus* (ATCC 29213), *Staphylococcus epidermidis* (ATCC 12228), *Enterococcus faecalis* (ATCC 29212), *Bacillus cereus* (ATCC 11778), *Escherichia coli* (ATCC 25922) and *Pseudomonas aeruginosa* (ATCC 27853). Bacteria were stored at –70 ºC and grown at 30 ºC on Columbia Agar with sheep blood (Oxoid, Wesel, Germany) suspended in physiological saline until an optical density of 0.1 AU (at 595 nm, 1 cm cuvette). The suspension was diluted (10 x) with physiological saline, and 2 μL of this inoculum was added to 100 μL growth medium, Nutrient Broth from Difco (ref. nr. 234000, lot nr. 6194895) with yeast extract (Oxoid LP 0021, lot nr. 900711, 2 g/400 mL broth) in microtiter plates (96 wells). All peptides including GS were dissolved in ethanol (4 g/L) and diluted in distilled water (1000 mg/L), and two–fold diluted in the broth (64, 32, 16, 8, 4 and 1 mg/L). incubation at 30 ºC (24 – 96 h) the MIC was determined as the lowest concentration inhibiting bacterial growth at 24h.

Hemolytic assays

Freshly drawn heparinized blood was centrifuged for 10 minutes at 1000*g* at 10 ºC, Subsequently, the erythrocyte pellet was washed three times with 0.85% saline solution and diluted with saline to a 1/25 packed volume of red blood cells. The peptides to be evaluated were dissolved in a 30% DMSO/0.5 mM saline solution to give a 1.5 mM solution of peptide. If a suspension was formed, the suspension was sonicated for a few seconds. A 1% Triton–X solution was prepared. Subsequently, 100 μl of saline solution was dispensed in columns 1–11 of a microtiter plate, and 100 μl of 1% Triton solution was dispensed in column 12. To wells A1–C1, 100 μl of the peptide was added and mixed properly. 100 μl of wells A1–C1 was dispensed into wells A2–C2. This process was repeated until wells A10–C10, followed by discarding 100 μl of wells A10–C10. These steps were repeated for the other peptides. Subsequently, 50 μl of the red blood cell solution was added to the wells and the

plates were incubated at 37 ºC for 4 h. After incubation, the plates were centrifuged at 1000g at 10 ºC for 4 min. In a new microtiter plate, 50 µl of the supernatant of each well was dispensed into a corresponding well. The absorbance at 405 nm was measured and the percentage of hemolysis was determined.

NMR spectroscopy:

^{1}H and ^{13}C–APT NMR for all intermediates (**18** and **19**) were recorded on a Bruker AV–400 (400/100 MHz). The spectra of the peptides (GS**4** and **11**) were recorded on a Bruker DMX 600 equipped with a pulsed field gradient accessory and a cryo–probe. For the 2D cROESY spectra (200 msec mixing time) the peptides were dissolved 7 mg/mL in 6% D_2O/H_2O mixture. Standard DQF–COSY (512c x 2084c) and TOCSY (400c x 2048c) spectra were recorded using presaturation for solvent suppression. cROESY[11] spectra (400c x 2048c, τ_{mix} = 180 ms) were recorded using the presat solvent suppression. All spectra were recorded in phase–sensitive mode, using either the TPPI or states–TPPI for quadrature detection in the indirect dimension. Homonuclear coupling constants were determined from the corresponding ^{1}H spectra.

N–2–pyridinil–*N*–2–(6–carbohydroxy)–pyridinil–urea (18)

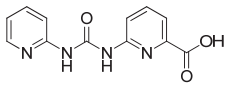

LC/MS: R_t 3.43 min, linear gradient 10→90% B in 13.5 min.; *m/z* = 258.93 $[M+H]^+$. IR: 3139.9, 2902.4, 1717.8, 1704.1, 1699.8, 1688.3, 1651.8 ; 1554.0, 1435.9, 1455.9, 1417.9, 1361.7, 1331.4, 1272.3, 1244.9, 1224.6, 1207.0, 1163.0, 1086.8, 1047.9, 1003.7. ^{1}H NMR (400 MHz, $(CD_3)_2SO$) δ 10.76 (br. s,.1H, N*H* urea), 8.34 (d, 1H, *J* = 4 Hz, C*H* pyridinil), 8.10 – 8.07 (m, 2H, J = 8.8, C*H* pyridinil), 7.92 (t, 1H, J = 8.8 Hz, C*H* pyridinil), 7.73 – 7.70 (m, 2H, C*H* pyridinil), 7.16 (dd, 1H, *J* = 6.0, 6.4, C*H* pyridinil), 4.22 (br. s., 1H, O*H*). ^{13}C NMR (151 MHz, $(CD_3)_2SO$) δ 166.10 (*C*=O), 152.46 (C_q pyridinil), 140.24, 119.80, 119.01, 116.43, 113.72 (*C*H pyridinil).

N–2–pyridinil–*N*–2–(6–(*tert*–butyl 2–ethylcarbamate) carbamido)–pyridinil–urea (19)

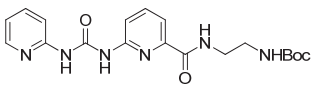

LC/MS: R_t 5.39 min, linear gradient 10→90% B in 13.5 min.; *m/z* = 400.93 $[M+H]^+$. IR: 3306.6, 2981.8, 1699.9, 1651.9, 1575.8, 1505.8, 1436.0, 1441.7, 1347.9, 1279.8, 1256.9, 1160.1, 1106.5, 1047.9. ^{1}H NMR (400 MHz, $(CD_3)_2SO$) δ 11.09 (br. s.,1H, N*H* urea), 10.28 (br. s,.1H, N*H* urea), 8.43 (t, *J* = 5.5 Hz, 1H, C*H* pyridinil), 8.37 (d, *J* = 4.3 Hz, 1H, C*H* pyridinil), 8.05 (d, *J* = 8.2 Hz, 1H, C*H* pyridinil), 7.95 (t, *J* = 7.9 Hz, 1H, C*H* pyridinil), 7.80 – 7.78 (m, 1H, C*H* pyridinil), 7.67 (d, *J* = 7.4 Hz, 1H, C*H* pyridinil), 7.56 (d, *J* = 7.8 Hz, 1H, C*H* pyridinil), 7.07 (dd, *J* = 6.8, 5.4 Hz, 1H), 6.97 (t, *J* = 5.4 Hz, 1H, C*H* pyridinil), 3.38 (q, *J* = 6.1, Hz, 2H), 3.17 (q, *J* = 5.8 Hz, 2H), 1.34 (s, 9H, *t*–butyl). ^{13}C NMR (151 MHz, $(CD_3)_2SO$) δ 163.76 (*C*=O), 152.36, 151.88, 151.17, 148.22 (C_q pyridinil), 139.73, 138.72, 118.03, 116.35, 115.35, 112.18 (*C*H pyridinil), 39.40 (CH_2), 28.15 (CH_3).

DAAD–Val–Orn–Leu–D–Phe–Pro–Val–Orn–Leu–ADDA (11)

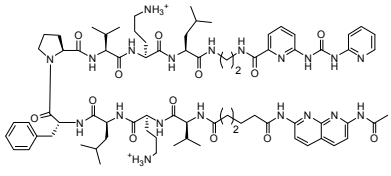

4–sulfamylbutyryl AM resin was preloaded with Fmoc–Leucine (loading tested with Fmoc test, 0.35 mmol/g). The resin was enlongated with automated SPPS in the amino acid order: Fmoc–Orn(Boc)–OH, Fmoc–Leu–OH, Fmoc–Pro–OH, Fmoc–D–Phe–OH, Fmoc–Leu–OH, Fmoc–Orn(Boc)–OH, Fmoc–Val–OH. DAAD template **17** (0.15 mmol, 55 mg) was activated with HCTU (0.15 mmol, 62 mg) and DiPEA (0.3 mmol, 50 µl) in NMP (4 ml) for 10 min. The mixture was added to the resin and shaken overnight. The resin was washed with NMP and DCM. Alkylation of the resin was achieved by addition of iodoacetonitril (280 µL)

and DiPEA (180 µL) via a syringe with basis alumina. The reaction mixture was covered with aluminium foil to protect it from light and it was shaken for 24 h at rt. The ADDA template **19** was first deporetected in 1:1 TFA/DCM. After full conversion the solvent was evaporated and the residue was coevaporated with toluene trice. ADDA template **20** was first dissolved in 20 % DiPEA in THF and subsequently added to the resin and stirred overnight at rt. The filtrate was collected and evaporated and the residue was applied to a Sephadex™ LH–20 size exclusion column (50.0 mmD x 1500 mmL) eluting with MeOH. After final deprotection of the Boc groups (95/2.5/2.5 TFA/TIS/H_2O) the product was purified by preparative HPLC (16.84 mg, 9.69µmol, 10%). LC/MS R_t 5.52 min, linear gradient 10→90% B in 13.5 min.; *m/z* = 1510.1 $[M+H]^+$. ^1H NMR (600 MHz, CD_3OH) *δ* 8.83 – 8.48 (m, 4H), 8.48 – 8.04 (m, 4H), 8.04 – 7.63 (m, 5H), 7.57 (s, 1H), 7.41 – 7.00 (m, 6H), 4.53 (tdd, *J* = 65.9, 14.5, 8.3 Hz, 2H), 4.38 – 4.25 (m, 1H), 4.12 (ddd, *J* = 28.7, 23.8, 8.4 Hz, 1H), 3.80 – 3.33 (m, 6H), 3.18 (dd, *J* = 10.2, 8.6 Hz, 1H), 3.11 – 2.82 (m, 6H), 2.74 – 2.41 (m, 2H), 2.37 – 1.21 (m, 24H), 1.10 – 0.63 (m, 27H). HRMS (ESI) m/z 1510.85212 $[M + H]^+$, 1510.85110 calcd. for $C_{76}H_{109}N_{20}O_{13}$

cyclo–[SAA4–Val–Orn–Leu–D–Phe–Pro–Val–Orn–Leu] 2·TFA:

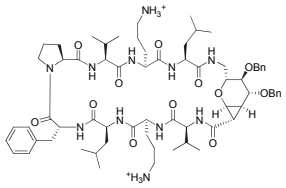

The octamer of gramicidin S was obtained via the procedure described in Chapter 2 (loading 0.31 mmol/g). Azido protected SAA**4** (63 mg, 1.5 eq.) was coupled to the octamer (326 mg, 0.31 mmol/g) with HCTU (62 mg, 1.5 eq) and DiPEA (3 eq., 50 µL). The same general procedure was followed as described in Chapter 2. The peptide was purified with RP–HPLC (linear gradient of 44–53%, 3 CV) to yield a white solid (24.0 mg, 16.1 µmol, 16%). ^1H NMR (600 MHz, CD_3OH) δ 8.71 (d, *J* = 5.1 Hz, 1H, NH ^{D}Phe$_5$), 8.53 (d, *J* = 6.7 Hz, 1H, N*H* Orn$_3$), 8.44 (d, *J* = 6.5 Hz, 1H, N*H* Val$_2$), 8.34 (d, *J* = 8.6 Hz, 1H, N*H* Orn$_8$), 8.30 (d, *J* = 8.0 Hz, 1H, N*H* Leu$_9$), 8.08 (d, *J* = 5.8 Hz, 1H, N*H* Val$_7$), 7.93 (d, *J* = 8.1 Hz, 1H, N*H* Leu$_4$), 7.73 (br. s, 2H, NH_2 Orn), 7.61 (t, *J* = 5.1 Hz, 1H, N*H* SAA), 7.36 – 7.25 (m, 15H), 4.85 – 4.82 (m, 2H), 4.70 (d, *J* = 12.0 Hz, 1H), 4.68 (d, *J* = 12.2 Hz, 1H), 4.61 (d, *J* = 11.8 Hz, 1H), 4.58 (d, *J* = 11.6 Hz, 1H), 4.59 – 4.57 (m, 1H, *H*α ^{D}Phe$_5$), 4.54 – 4.52 (m, 1H, *H*α Leu$_4$), 4.49 – 4.46 (m, 1H, *H*α Orn$_8$), 4.45 – 4.41 (m, 1H, *H*α Leu$_9$), 4.41 – 4.37 (m, 1H, *H*α Orn$_3$), 4.35 (dd, *J* = 8.4, 3.1 Hz, 1H, *H*α Pro$_6$), 3.95 (t, *J* = 7.1 Hz, 1H, *H*α Val$_2$), 3.87 (dd, *J* = 8.3, 6.3 Hz, 1H, *H*α Val$_7$), 3.79 – 3.70 (m, 4H), 3.65 (s, 1H), 3.54 – 3.52 (dd, 1H, J = 7.1, 1.2 Hz), 3.40 (t, J = 4.5 Hz, 1H), 3.14–3.11 (m, 1H), 2.99–3.01 (m, 2H), 2.97–2.92 (m, 4H), 2.90–2.87 (m, 1H), 2.82 (dd, *J* = 17.3, 8.2 Hz, 1H), 2.13 – 2.01 (m, 4H), 2.01 – 1.88 (m, 4H), 1.88–1.80 (m, 2H), 1.80 – 1.70 (m, 7H), 1.70 – 1.55 (m, 8H), 1.51–1.47 (m, 2H), 1.44 – 1.36 (m, 2H), 1.33 (s, 1H), 1.31 – 1.27 (m, 1H), 1.05 (d, *J* = 6.7 Hz, 3H), 1.03 (d, *J* = 6.7 Hz, 3H), 1.01 (d, *J* = 6.9 Hz, 3H), 0.95 – 0.93 (m, 6H), 0.94 (d, *J* = 1.9 Hz, 3H), 0.90 (d, *J* = 4.3 Hz, 3H), 0.89 (d, *J* = 5.0 Hz, 3H), 0.85 (d, *J* = 6.5 Hz, 3H).^{13}C NMR (151 MHz, CD_3OH) δ 174.45, 174.39, 174.09, 173.86, 173.68, 173.38, 173.04, 172.85, 139.46, 139.35, 137.52, 130.49, 129.71, 129.54, 129.50, 129.20, 129.06, 128.96, 128.95, 128.41, 78.23, 75.89, 73.86, 72.57, 68.17, 62.21, 61.53, 61.38, 55.42, 53.81, 53.51, 52.32, 49.72, 48.32, 40.83, 40.74, 37.98, 31.13, 30.93, 30.51, 27.51, 26.08, 25.64, 25.28, 24.84, 24.09, 23.46, 23.43, 22.59, 21.80, 19.86, 19.81, 19.76, 19.29.HRMS (ESI) *m/z* 1262.75695 $[M + H]^+$, 1262.75474 calcd. for $C_{68}H_{100}N_{11}O_{12}$; LC/MS: R_t 7.65 min, linear gradient 10→90% B in 13.5 min.; *m/z* = 1262.7 $[M+H]^+$.

References

[1] Knijnenburg, A.D.; Tuin, A.W.; Spalburg, E.; de Neeling, A.J.; Mars–Groenendijk, R. H.; Noort, D.; Otero, J. M.; Llamas–Saiz, A. L.; van Raaij, M. J.; van der Marel, G. A.; Overkleeft, H. S.; Overhand, M.; *Chem. Eur. J.*, **2011**, *17*, 3995.

[2] (a) Jelokhani–Niaraki, M.; Hodges, R. S.; Meissner, J. E.; Hassenstein, U. E.; Wheaton, L. *Biophys. J.* **2008**, *95*, 3306. (b) Jelokhani–Niaraki, M.; Kondejewski, L. H.; Farmer, S. W.; Hancock, R. E. W. *Biochem. J.* **2000**, *349*, 747.

[3] Knijnenburg, A. D.; Spalburg, E.; de Neeling, A. J.; Mars–Groenendijk, R. H.; Noort, D.; Grotenbreg, G. M.; van der Marel, G. A.; Overkleeft, H. S.; Overhand, M. *ChemMedChem* **2009**, *4*, 1976.

[4] Knijnenburg, A. D.; Kapoerchan, V. V.; Grotenbreg, G. M.; Spalburg, E.; de Neeling, A. J.; Mars–Groenendijk, R. H.; Noort, D.; Otero, J. M.; Llamas–Saiz, A. L.; van Raaij, M. J.; Ravensbergen, B.; Nibbering, P. H.; van der Marel, G. A.; Overkleeft, H. S.; Overhand M., *Bioorg. Med. Chem.* **2011**, 19, 3402.

[5] (a) Semrau, S.; Monster, M. W. L.; van der Knaap, M.; Florea, B. I.; Schmidt, T.; Overhand, M. *Biochim. Biophys. Acta* **2010**, *1798*, 2033. (b) Kiricsi, M.; Prenner, E. J.; Jelokhani–Niaraki, M.; Lewis, R. N. A. H.; Hodges, R. S.; McElhaney, R. N. *Eur. J. Biochem.* **2002**, *269*, 5911.

[6] Ando, S.; Takiguchi, H.; Izumiya, N. *Bull. Chem. Soc. Jpn.* **1983**, *56*, 3781.

[7] (a) Corbin, P. S.; Zimmerman, S. C.; Thiessen, P. A.; Hawryluk, N. A.; Murray, T. J. *J. Am. Chem. Soc.* **2001**, *123*, 10475; (b) Lüning, U.; Kühl, C.; Uphoff, A. *Eur. J. Org. Chem.* **2002**, 4063. (c) Pauling, L.; Pressman, D. *J. Am. Chem. Soc.* **1945**, 67, 1003. (d) Adrian, J. C.; Wilcox, C. S. *J. Am. Chem. Soc.* **1992**, *114*, 1398.

[8] (a) Epand, R. M.; Epand, R. F. *Biochim. Biophys. Acta* **2009**, *1788*, 289. (b) van Meer, G.; Voelker, D. R.; Feigenson, G. W. *Nature Rev. Mol. Cell Biol.* **2008**, *9*, 112.

[9] Unpublished results W. L. van der Linden

[10] (a) Blanco, F. J.; Jimenez, M. A.; Pineda, A.; Rico, M.; Santoro, J.; Nieto, J. L. *Biochemistry* **1994,** *33*, 6004. (b) Cagas, P. M.; Corden, J. L. *Prot–Struct. Funct. Gen.* **1995**, *21*, 149.

[11] Griesinger C.; Ernst, R. R. *J. Magn. Reson.* **1987**, *75*, 261.